Structural and Functional Characterization of Anticoagulant, FXa-binding *Viperidae* Snake Venom Phospholipases A$_2$

Grazyna Faure* and Frederick Saul

Institut Pasteur, Unité d'Immunologie Structurale; CNRS, URA 2185, Département de Biologie Structurale et Chimie, 25, rue du Dr. Roux F-75015, Paris, France

* *Corresponding author: E-mail: grazyna.faure-kuzminska @pasteur.fr*

Dedicated to the memory of Professor Franc Gubenšek

Abstract

Certain snake venom phospholipases A$_2$ (PLA$_2$) have been identified as specific, non-competitive blood coagulation inhibitors that bind with high affinity to human activated blood coagulation factor X (hFXa). Recent determination of the three-dimensional structures of PLA$_2$ isoforms which differ in anticoagulant activity contributes to a better understanding of their mode of binding to human FXa. Detailed analysis of the crystal structures of natural PLA$_2$ isoforms from *Viperidae* snake venom which differ in binding affinity to hFXa allows us to detect local conformational changes and precisely delineate the role of critical residues in the anticoagulant function of these PLA$_2$. We find conformational changes at conserved position Lys127 and mutated position Lys128 > Glu in the C-terminal regions of less potent anticoagulant PLA$_2$ (AtxC and CBa$_2$), which contribute to the observed decrease in affinity for hFXa. The mutation His1 > Ser in less potent CBa$_2$ is associated with a significant displacement of the side chain of Lys69 and Trp70 in the loop 65–72 and could also explain the reduced anticoagulant activity of the CBa$_2$-FXa complex. Knowledge of the spatial arrangement of the sites of interaction of PLA$_2$ with hFXa is important for understanding of the hemostatic process at the molecular level and could provide new anticoagulant drug leads.

Keywords: Snake venom anticoagulant phospholipases A$_2$; coagulation factor Xa; anticoagulant site; SPR affinity; crystal structure

1. Introduction

Snake venom PLA$_2$ (sPLA$_2$, EC 3.1.1.4) are interfacial enzymes which bind to the cell membrane surface and catalyze hydrolysis of the 2-acyl ester bond of 1,2-diacyl-3-*sn*-phosphoglycerides.[1] These small disulfide-rich enzymes (13–18 kDa) also selectively interact with various targets such as phospholipids (PL), proteins and heparan sulfate proteoglycans. Interestingly, individual snake venom contains several PLA$_2$ isoforms which differ in enzymatic activity and toxic effects.[2–3] The presence of various PLA$_2$ isoforms with diverse pharmacological activities could be explained by accelerated evolution of exon regions after duplication of a common ancestral gene, indicating rapid adaptation of snakes for defense and predation.[4] Although the catalytic site (residues His48, Asp99, Tyr52, Tyr73),

the Ca^{2+}-binding loop, and the interfacial binding surface (IBS), as well as intra-chain disulfide bonds and the overall 3D-structure of snake venom PLA$_2$ groups I and II are highly conserved, small differences in exposed surface residues could play an important role in determining functional specificities.

In addition to their catalytic function, snake venom PLA$_2$ exhibit diverse activities including neurotoxic, myotoxic, myonecrotic, anticoagulant, convulsant, hypotensive and oedema-inducing activities.[5–9] Bactericidal, antitumoral, anti-HIV, anti-*Leishmania*, and anti-*Plasmodium* activity have also been reported.[10–12] Interactions with various protein targets determine the specific function of PLA$_2$ (*i.e.* neurotoxic, anti-coagulant or other activities). The presence of pharmacologically distinct sites independent of the catalytic site was first proposed by Kini.[13] Increasing experimental evidence has shown that the vari-

ous receptor-mediated functions of PLA$_2$s may be either dependent or independent of their enzymatic activity.[13–17] The molecular mechanism and structural basis by which the PLA$_2$s, with a highly conserved three-dimensional scaffold, exhibit diverse biological functions are still to be elucidated. In this short review, we analyse by structural and functional studies, several *Viperidae* venom sPLA$_2$s that exert an anticoagulant effect by a non-enzymatic PL-independent mechanism through direct binding to hFXa.[18–21] Other mechanisms by which PLA$_2$ may inhibit the coagulation process have been recently reviewed.[17,22]

Factor Xa plays a central role in the coagulation cascade, converting prothrombin to thrombin by limited proteolysis, and is essential for the blood clotting process.[23] FXa contains two polypeptide chains linked by a single interchain disulfide bond. The light chain consists of an N-terminal Gla domain containing post-translationally modified $\bar{\gamma}$-carboxyglutamate residues and two epidermal growth factor-like (EGF-like) domains. The heavy chain, which contains a serine protease catalytic domain, consists of two subdomains of antiparallel β-barrel structure each comprising a β-sheet of six strands and four α-helices. Residues His236, Asp282 and Ser379 form a catalytic triad at the active site cleft between the two subdomains.

Thrombosis occurs in a variety of cardiac disorders and a search for new, non-competitive FXa inhibitors with high selectivity is challenging. The anticoagulant FXa-

binding sPLA$_2$ present a novel family of agents useful in identifying the site of interaction of anticoagulants at the level of specific amino acid residues and could provide a promising structural template for the 3D structure-based design of new, non toxic hFXa inhibitors.

2. Structural Scaffold and Anticoagulant Properties of FXa-binding PLA$_2$

FXa-binding PLA$_2$s of the *Viperidae* family, such as myotoxin II (MtxII) from *Bothrops asper*, two isoforms of the basic CB subunit (CBc and CBa$_2$) of the crotoxin complex from *Crotalus durissus terrificus*, two isoforms of ammodytoxin (AtxA and AtxC) from *Vipera ammodytes ammodytes*, the basic subunit (CbII) of the CbICbII complex from *Pseudocerastes fieldi*, the basic PLA$_2$ from *Agkistrodon halys pallas* (bAhp) and *Daboia russelli pulchella* (DPLA$_2$) are basic enzymes with a molecular weight of 13–17 kDa containing seven conserved disulfide bonds. Their sequences with secondary structure elements (helices A,B,C, D and the β-wing) are presented in Figure 1, showing the conserved 25–33 Ca^{2+} binding loop and the catalytic diad residues His48 and Asp99.[24–25] The IBS is formed by a hydrophobic channel[1,26] surrounding the en-

```
        ___helix A___   _helix B_   _Ca²⁺-loop_   ___helix C___

MtxII   SLFELGKMIL QETGKNPAKS YGAYGCNCGV LGRGKPKDAT DRCCYVHKCC YKKLTGCNPK
CBc     HLLQFNKMIK FETRKNAIPF YAFYGCYCGW GGRGRPKDAT DRCCFVHDCC YGKLAKCNTK
AtxA    SLLEFGMMIL GETGKNPLTS YSFYGCYCGV GGKGTPKDAT DRCCFVHDCC YGNLPDCSPK
CBa2    SLLQFNKMIK FETRKNAVPF YAFYGCYCGW GGQGRPKDAT DRCCFVHDCC YGKLAKCNTK
CbII    NLFQFTKMIN GKLGAFAVLN YISTGCYCGW GGQGTPKDAT DRCCFVRDCC YGRVKGCNPK
AtxC    SLLEFGMMIL GETGKNPLTS YSFYGCYCGV GGKGTPKDAT DRCCFVHDCC YGNLPDCSPK
bAhp    HLLQFRKMIK KMTGKEPVVS YAFYGCYCGS GGRGKPKDAT DRCCFVHDCC YEKVTGCDPK
DPLA2   SLLEFGKMIL EETGKLAIPS YSSYGCYCGW GGKGTPKDAT DRCCFVHDCC YGNLPDCNPK
AGTX    NLLQFNKMIK EETGKNAIPF YAFYGCYCGW GGQGKPKDGT DRCCFVHDCC YGRLVNCNTK


        ___β-wing___   ____helix D____   __C-terminal region__

MtxII   KDRYSYSWKD KTIVCGENNS CLKELCECDK AVAICLRENL NTYNKKYRYY LKPLCK-KAD AC
CBc     WDIYPYSLKS GYITCGKGTW CEEQICECDR VAAECLRRSL STYKYGYMFY PDSRCRGPSE TC
AtxA    TDRYKYHREN GAIVCGKGTS CENRICECDR AAAICFRKNL KTYNYIYRNY PDFLCKKESE KC
CBa2    WDIYRYSLKS GYITCGKGTW CKEQICECDR VAAECLRRSL STYKNEYMFY PDSRCREPSE TC
CbII    LAIYSYSFQK GNIVCGKNNG CLRDICECDR VAANCFHQNK NTYNRNYRFL SSSRCRQTSE QC
AtxC    TDRYKYHREN GAIVCGKGTS CENRICECDR AAAICFRKNL KTYNYIYRNY PDILCKEESE KC
bAhp    WDDYTYSWKN GTIVCGGDDP CKKEVCECDK AAAICFRDNL KTYKKRYMAY PDILCSSKSE KC
DPLA2   SDRYKYKRVN GAIVCEKGTS CENRICECDK AAAICFRQNL NTYSKKYMLY PDFLCKGEL- KC
AGTX    SDIYSYSLKE GYITCGKGTN CEEQICECDR VAAECFRRNL DTYNNGYMFY RDSKCTETSE EC
```

Figure 1: Amino-acid sequences of FXa-binding PLA$_2$ from *Viperidae* venom. MtxII: myotoxin II from *Bothrops asper* (PDB 1CLP); CBc and CBa$_2$: isoforms of the basic subunit of the crotoxin complex from *Crotalus durissus terrificus* (PDB 2QOG); AtxA and AtxC: isoforms of ammody-toxin from *Vipera ammodytes ammodytes* (PDB 3G8G and 3G8H, respectively); CbII: basic subunit of the CbICbII complex from *Pseudocerastes fieldi*;[39] bAhp: basic PLA$_2$ from *Agkistrodon halys pallas* (PDB 1JIA); DPLA$_2$: basic PLA$_2$ from *Daboia russelli pulchella* (PDB 1ZWP) and AGTX: agkistrodotoxin, a neutral PLA$_2$ from *Agkistrodon halys pallas* (PDB 1BJJ) used as a negative control for absence of FXa-binding. Strictly conserved residues, including the catalytic site, are underlined.

trance to the active site and contains a ring of cationic and hydrophobic residues which make contact with lipid during association of PLA$_2$ with the membrane surface.[16]

The crystal structures of PLA$_2$ analyzed here have been previously determined (the PDB accession codes are shown in Table 1). These sPLA$_2$ from *Viperidae* snake venom are structurally homologous to the inflammatory, non-pancreatic mammalian sPLA$_2$ of group IIA which also exhibit anticoagulant activity by interacting with FXa.[18] Figure 2a shows the canonical structural features of group IIA PLA$_2$s for the case of AtxA, which was solved in our laboratory in collaboration with the group of Igor Križaj (Institute Jožef Stefan, Ljubljana).[27] The structure contains an N-terminal α-helix (A), a short helix (B),
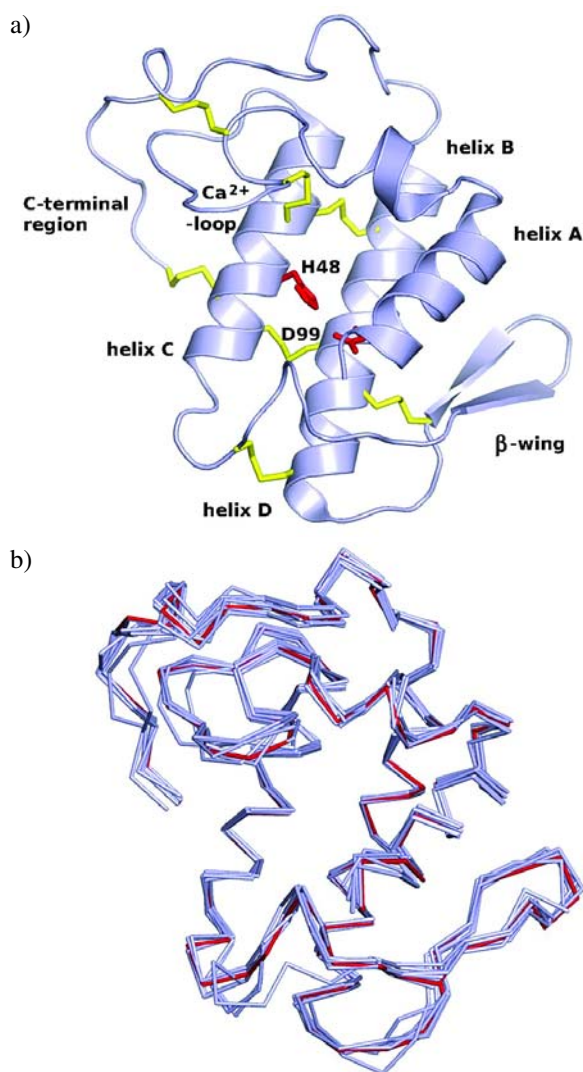

a)

b)

Figure 2: Overall structure of group IIA PLA$_2$ from *Viperidae* venom which interact with FXa. (**a**) The crystal structure of AtxA (PDB 3G8G)[27] shown in the classical front face orientation. The catalytic diad (residues His48/Asp99) are shown in red and the seven conserved disulfide bonds are in yellow. (**b**) The superimposed structures of seven FXa-binding PLA$_2$ (shown in blue) and AGTX (PDB 1BJJ, negative control, shown in red).

a Ca^{2+}-binding loop, a long α-helix (C), an anti-parallel two-stranded beta sheet (β-wing), a long α-helix (D) anti-parallel to helix C, and an extended C-terminal region. Two anti-parallel disulfide-linked α-helices (C and D) form a rigid scaffold to which the Ca^{2+}-binding loop, the C-terminal loop and the β-wing are covalently linked by disulfide bonds. The highly conserved active site residues His48, Asp99, Tyr52, are clustered on helices C and D and interact via Asp49 with the Ca^{2+}-binding loop.[17,27]

All PLA$_2$ presented in Figure 1 inhibit formation of the prothrombinase complex. Several studies have proposed that FXa-binding PLA$_2$ compete with factor Va for the FXa-binding site, introducing a lag time in the production of thrombin.[18–21,28–31] The binding affinities between these group IIA sPLA$_2$ from *Viperidae* snake venom and FXa, and their inhibition of prothrombinase activity are presented in Table 1. These results show a strong correlation between the dissociation constant K_d^{app} and prothrombinase inhibition, and allow the classification of anticoagulant PLA$_2$ into three groups displaying strong, medium and weak anticoagulant activity, respectively (Table 1)[21].

Table 1. SPR kinetic parameters of FXa-binding PLA$_2$ and their effect on prothrombinase activity.

PLA$_2$	k_{on} (M^{-1}s^{-1})	k_{off} (s^{-1})	K_d^{app} (nM)	IC$_{50}$ (nM)	PDB
MtxII	10. 4 × 10^6	1. 78 × 10^{-2}	1. 8	3	1CLP
CBc	3. 2 × 10^5	1. 6 × 10^{-4}	0. 6	0. 7	2QOG
AtxA	2. 2 × 10^5	7. 0 × 10^{-3}	30	25	3G8G
CBa$_2$	2. 9 × 10^5	1. 5 × 10^{-2}	52	41	2QOG
CbII	4. 2 × 10^5	8. 5 × 10^{-3}	20	20	–
AtxC	3. 9 × 10^4	1. 4 × 10^{-2}	346	240	3G8H
bA*hp*	4. 0 × 10^4	1. 6 × 10^{-2}	400	90	1JIA
DPLA$_2$	4. 5 × 10^4	2. 6 × 10^{-2}	578	130	1ZWP
AGTX	NB	NB	NB	> 10^4	1BJJ

Kinetic parameters of FXa-binding PLA$_2$ and effects on prothrombinase activity.[20–21] K_d^{app} = k_{off}/k_{on} determined by SPR. IC$_{50}$ corresponds to 50% inhibition of thrombin generation in the absence of phospholipids for the different PLA$_2$s. NB: non-binding. The protein data bank access code for each structure is shown.

Figure 2b shows the superposition of the α-carbon backbone of agkistrodotoxin (AGTX, a neutral PLA$_2$ from *Agkistrodon halys pallas* used as negative control for absence of FXa binding) with the crystal structures of the FXa-binding PLA$_2$ presented in Figure 1. AGTX displays a 3D profile similar to the FXa-binding PLA$_2$. Small variations in the topology of the C-terminal region and the loop preceeding the β-wing are observed for all FXa-binding PLA$_2$. The electrostatic charge distribution in FXa-binding PLA$_2$ suggests that small differences in conformation and charge might have functional significance. Comparison of the 3D structures of different sPLA$_2$ and their isoforms, together with mutagenesis and affinity-

binding studies, could help to understand the role of the mutated residues in the anticoagulant function of FXa-binding PLA$_2$.

3. Search for the Anticoagulant Site of FXa-binding PLA$_2$

To date, co-crystallisation experiments of PLA$_2$ with FXa have been unsuccessful, and elucidation of the three-dimensional structure of the PLA$_2$-FXa complex presents a major challenge. Various approaches have been used to
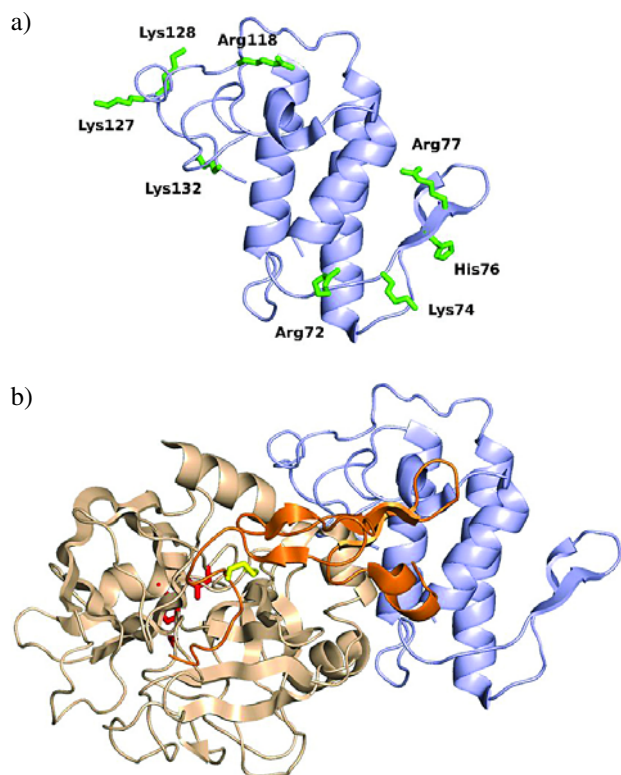
a)

b)

Figure 3: FXa-binding site of AtxA (**a**) and three-dimensional molecular model of the PLA$_2$-FXa complex obtained by molecular docking (**b**).

(a) Crystal structure of AtxA[27] showing residues (in green) previously identified as important for binding to FXa and anticoagulant activity.[20]

(b) The 3D molecular model of the complex shows the contact interface between the two molecules.[21] The light chain of hFXa (PDB 2BOH, without the Gla- and EGF-like1 domains) is shown in orange and the heavy chain is shown in brown. The catalytic triad His236 (His[57])/Asp282 (Asp[102])/Ser379 (Ser[195]) (the chymotrypsinogen numbering is shown with residue numbers in superscript) is in red and the single disulfide bridge linking the light and heavy chains is shown in yellow. The structure of AtxA (shown in blue) in the complex is oriented as in Figure 2a. The docking model shown here[21] does not include the EGF-like domain-1, which is not visible in the crystal structure of hFXa. However, we predicted that the β-wing will be in contact with the EGF-like 1 domain considering the model of hFXa by Bajaj and coworkers[34] based on homology with the crystal structure of porcine FIXa.[35]

study the structure-function relationship of anticoagulant PLA$_2$ with hFXa: site–directed mutagenesis, molecular docking, affinity binding studies, physiological tests for inhibition of prothrombinase activity, and comparison of crystallographic structures of natural PLA$_2$ isoforms which differ in binding affinity for FXa.

By site-directed mutagenesis and SPR affinity binding studies we demonstrated the importance of basic residues Arg72, Lys74, His76,Arg77 in the β-wing and Arg118, Lys128, Lys127, Lys132 in the C-terminal region, for binding of AtxA to FXa (Figure 3A).[20]

Using molecular docking simulations between PLA$_2$ and FXa, we have mapped the interaction sites on *Viperidae* snake venom PLA$_2$s and hFXa.[21] Figure 3B shows the three-dimensional molecular model of the AtxA-FXa complex obtained by molecular docking. We proposed that the potential FXa-binding site for PLA$_2$ comprises two adjacent regions: region A (residues 1–19 and 52–77), which includes solvent-exposed residues of helices A and B and part of the loop between helix C and the β-wing, and region B (residues 23–34 and 118–133), which corresponds to the Ca^{2+} binding loop and the C-terminal region.[21]

Interestingly, residues 52–77 of the PLA$_2$ proposed here as one of the regions important for FXa-binding, have previously been identified as the putative positively charged anticoagulant site of the PLA$_2$s exerting pharmacological effect through binding to anionic PL during the anticoagulation process.[13,18,32] Previously, it was suggested that a glutamic acid residue in position 53 may be important for anticoagulant activity.[33] However, in the FXa-binding PLA$_2$, shown in Figure 1, position 53 is occupied by glycine or lysine (the only exception is bAhp which displays weak FXa-binding activity). These differences suggest that anticoagulant mechanisms such as binding to anionic PL or binding to FXa involve different residues in the anticoagulant site.

Surface Plasmon Resonance (SPR) studies using whole FXa and FXa without the Gla-domain show similar affinity for immobilized PLA$_2$, indicating that the N-terminal Gla domain is not important for PLA$_2$-FXa interaction.[21] Molecular docking calculations indicated that the potential PLA$_2$ binding site of FXa is composed of five regions of the heavy chain and two segments of the EGF-like 2 domain of the light chain.[21,17] The PLA$_2$ catalytic site and FXa catalytic site are accessible and not involved in the binding interface.

The importance of the β-wing and C-terminal regions (Figure 3A) of PLA$_2$ for binding to FXa is based on mutagenesis experiments.[20] The molecular docking model (Figure 3B) is based on mutagenesis data and on the hFXa structure (PDB 2BOH, which does not include the EGF-like domain-1 not visible in the crystal structure). However, we predicted that the β-wing can make contact with the EGF-like 1 domain considering the model of hFXa by Bajaj and coworkers,[34] which includes the EGF-

like 1 domain based on homology with the structure of porcine FIXa.[35] The orientation of the EGF-like domain 1 in this model allows contact with the β-wing region of PLA$_2$.

In addition, an exosite which binds heparin in the heavy chain of FXa is probably important for interaction with anticoagulant PLA$_2$.[17] Interestingly, a particular structural motif of FXa (residues 233–243 in the C-terminal region of the heavy chain), important for binding of anticoagulant protein NAPc2 from the hematophagous nematode *Ancylostoma caninum* (PDB 2H9E), is also important for interaction with anticoagulant PLA$_2$.

By analysing the crystallographic structures of anticoagulant PLA$_2$ isoforms which differ in binding affinity to hFXa, we aim to detect local conformational changes which occur in these natural isoforms and precisely delineate the role of critical residues in the anticoagulant function of PLA$_2$. In particular, we have compared the crystal structures of isoforms AtxA and AtxC of ammody-

toxin, which differ in sequence by only two amino-acid substitutions (Phe124 > Ile and Lys128 > Glu) but display significant differences in toxicity and anticoagulant activity.[27] The crystal structures allow us to explain the 10-fold decrease in binding affinity of AtxC for FXa (Table 1). Briefly, the side chain of Lys128 in AtxA (residue identified by mutagenesis as important for interaction with FXa)[20] is fully exposed and accessible for binding to FXa, whereas the side chain of Glu128 in AtxC makes a stabilizing hydrogen bond with the main chain nitrogen atom of Thr35, leading to reorientation of the polypeptide chain backbone at positions 127 and 128 and a significant shift in the side chain of the conserved residue Lys127.[27] Lys127 has been identified by mutagenesis as important for the interaction of AtxA with FXa[20] and has been identified by molecular docking calculations as part of the anticoagulant site.[21]

We find similar conformational changes at position 127 and 128 in isoforms CBc and CBa$_2$ of the basic subu-
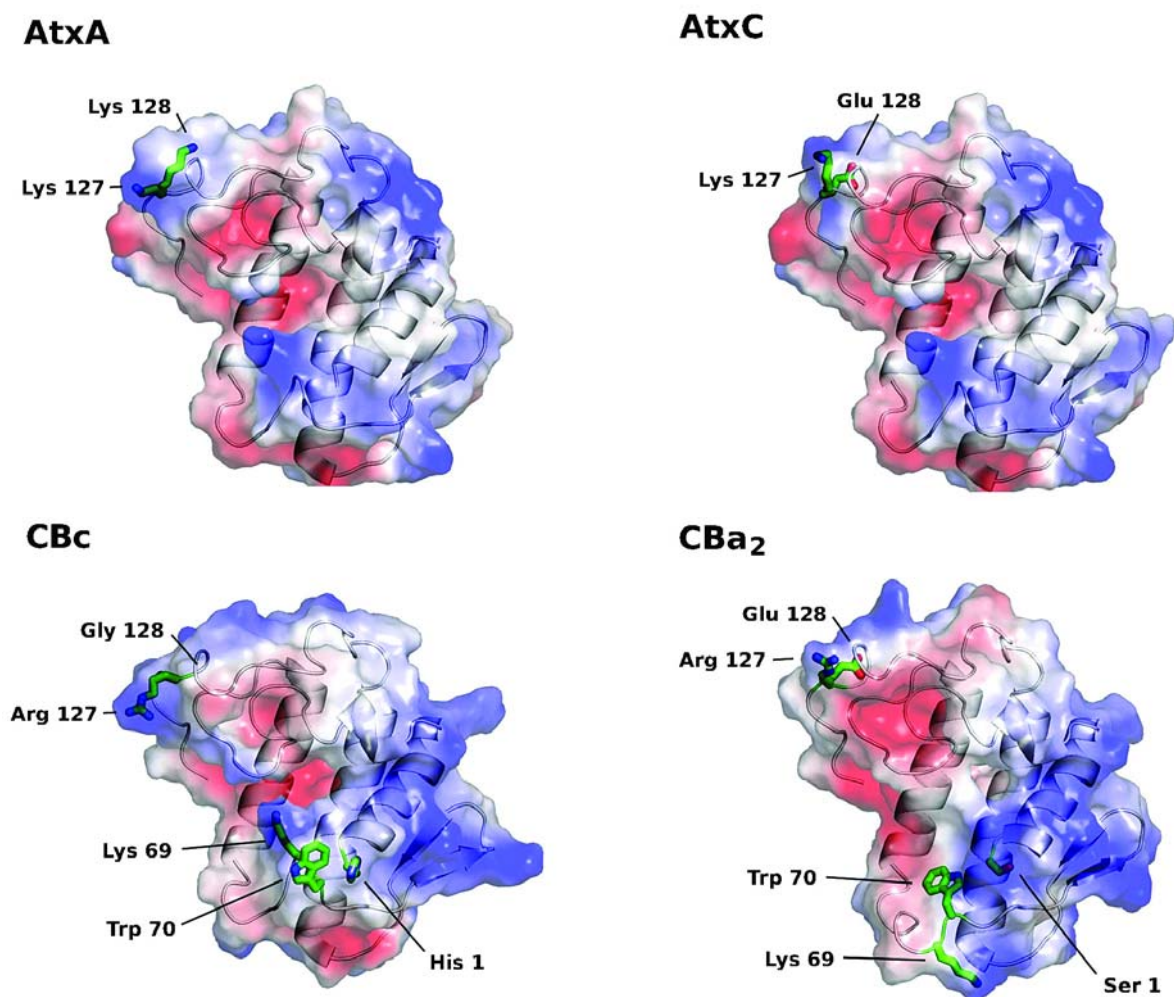
Figure 4: Crystallographic structures of PLA$_2$ isoforms AtxA, AtxC, CBc and CBa$_2$ showing critical residues responsible for differences in anticoagulant activity. The mutations Lys128 > Glu in AtxC and Gly128 > Glu in CBa$_2$ lead to a significant decrease in binding affinity for FXa. The additional mutation His1 > Ser in CBa$_2$, leading to a displacement of Trp70 and Lys69, could also be responsible for the decreased binding affinity for hFXa.

nit of crotoxin from *Crotalus durissus terrificus*. The pharmacological properties of these individual CB isoforms have been previously reported.[36–37] Isoforms CBc and CBa$_2$ differ in sequence by eight substitutions (His1 > Ser, Ile18 > Val, Gln33 > Arg, Pro65 > Arg, Glu82 > Lys; Tyr105 > Asn, Gly106 > Glu and Gly117 > Glu) and differ significantly in binding affinity to FXa (CBa$_2$ displays 100-fold lower affinity for FXa and 60-fold lower anticoagulant activity) (Table 1).[21] Since the crystal structure of a tetrameric complex formed by a mixture of isoforms CBc and CBa$_2$ has been reported,[38] we compared the structures of these individual CB isoforms with the structures of AtxA and AtxC. We concluded that, similarly to the structure of AtxC, the mutation in position 128 in CBa$_2$ leads to a shift in the side chain of unmutated Arg127 (Lys127 in AtxC) due to interaction between Glu128 and the main chain nitrogen atom of residue 35 (Arg 35 in CBa$_2$), and displacement of the main polypeptide chain at positions 127–128 contributing to the observed decrease in affinity for FXa.[17] The conserved residues at position 127 in both isoforms of ammodytoxin and subunit CB display different conformations detectable only by comparison of the 3D structures.

Moreover, by comparing the superimposed structures of CBc and CBa$_2$ we detected important structural differences in the N-terminal region adjacent to the loop preceeding the β-wing (Figure 4). The mutation His1 > Ser in CBa$_2$ is associated with a significant displacement of the side chains of Lys 69 and Trp70 in the loop 65–72. These conformational differences could inhibit interaction with FXa and thus explain the reduced anticoagulant activity observed for the CBa$_2$-FXa complex (Figure 4 and Table 1). The electrostatic charge distribution and molecular surface in this region differ significantly (Figure 4).

4. Conclusions and Remarks

In this review we analyse the structure and function of several *Viperidae* venom sPLA$_2$s that exert an anticoagulant effect by a non-enzymatic, PL-independent mechanism through direct binding to human FXa. Precise knowledge of the crystallographic structures of PLA$_2$ isoforms and their functional properties allows us to detect conformational differences of residues important for interaction with FXa and to show the local effects induced by natural mutations. The significantly reduced anticoagulant activity of AtxC and CBa$_2$ is due to the lower binding affinity for FXa resulting from the mutation Glu128 > Lys. Additionally, the mutation His1 > Ser in CBa$_2$ is associated with a displacement of Lys69 and Trp70 compared with isoform CBc, which could also inhibit interaction with FXa. Further structural studies involving crystallization of the complex are required to provide a detailed view of the PLA$_2$-FXa interface and confirm our proposal for the anticoagulant site.

5. References

1. O. G. Berg, M. H. Gelb, M. D. Tsai, M. K. Jain, *Chem. Rev.* **2001**, *101*, 2613–2653.
2. G. Faure, C. Bon, *Toxicon* **1987**, *25*, 229–234.
3. G. Faure, C. Bon, *Biochemistry* **1998**, *27*, 730–738.
4. D. Kordiš, F. Gubenšek, *Eur. J. Biochem.* **1996**, *240*, 83–90.
5. R. M. Kini, in: R. M. Kini, (Ed.): Venom Phospholipases A$_2$ Enzymes: Structure, Function and Mechanism, Chichester: Wiley, **1997**, pp 1–28.
6. R. M. Kini, *Toxicon* **2003**, *42*, 827–840.
7. E. Valentin, G. Lambeau, *Biochimie* **2000**, *82*, 815–31.
8. J. M. Gutierrez, B. Lomonte, *Toxicon* **1995**, *33*, 1405–1424.
9. C. L. Ownby, *J. Toxicol. -Toxins Rev.* **1998**, *17*, 213–238.
10. T. J. Nevalainen, G. G. Graham, K. F. Scott, *Biochem Biophys Acta* **2008**, *1781*, 1–9.
11. D. Fenard, G. Lambeau, E. Valentin, J. C. Lefebvre, M. Lazdunski, A. J. Doglio, *Clin. Invest.* **1999**, *104*, 611–618.
12. H. Zieler, D. B. Keister, J. A. Dvorak, J. M. Ribeiro, *J. Exp. Biol.* **2001**, *204*, 4157–4167.
13. R. M. Kini, H. J. Evans, *Toxicon* **1989,** *27*, 613–635.
14. R. Doley, R. M. Kini, *Cell. Mol. Life Sci.* **2009,** *66*, 2851–5871.
15. G. Faure, in: F. Goudey-Perrière, C. Bon, S. Puiseux-Dao, Sauviat, M. (Eds): Toxines et recherches biomédicales. SFET collection, "Rencontres en toxinologie", Elsevier, Paris, France, **2002,** pp. 305–313.
16. L. Chioato, R. J. Ward, *Toxicon*, **2004,** *42*, 869–883.
17. G. Faure, H. Xu, F. Saul, in: R. M. Kini, K. Clemetson, F. S. Markland, M. A. McLane, Morita, T. (Eds): Toxins and Hemostasis: From Bench to Bedside, Springer Science+Business Media B. V. Dordrecht Heidelberg London New York, **2010**, pp. 201–217.
18. C. M. Mounier, T. M. Hackeng, F. Schaeffer, G. Faure, C. Bon, J. H. Griffin, *J. Biol. Chem.* **1998**, *273*, 23764–23772.
19. R. T. Kerns, R. M. Kini, S. Stefansson, H. J. Evans, *Arch Biochem. Biophys.* **1999**, *369*, 107–113.
20. P. Prijatelj, M. Charnay, G. Ivanovski, Z. Jenko, J. Pungerčar, I. Križaj, G. Faure, *Biochimie* **2006**, *88,* 69–76.
21. G. Faure, V. T. Gowda, R. Maroun, *BMC-Struct. Biol.* **2007**, 7:82. http://www.biomedcentral.com/1472-6807/7/82
22. T. Sajevic, A. Leonardi, I. Križaj, *Toxicon* **2011**, *57*, 627–645.
23. E. W. Davie, *Throm. Hoemost.* **1995,** *74*, 1–6.
24. D. L. Scott, S. P. White, Z. Otwinowski, W. Yuan, M. H. Gelb, P. B. Sigler, *Science* **1990**, *250*, 1541–1546.
25. R. K. Arni, R. J. Ward, *Toxicon*, **1996**, *34*, 827–841.
26. Y. Snitko, R. S. Koduri, S. K. Han, R. Othman, S. F. Baker, B. J. Molini, D. C. Wilton, M. H. Gelb, W. Cho, *Biochemistry* **1997**, *36*, 14325–14333.
27. F. A. Saul, P. Prijatelj-Žnidaršič, B. Vuillez-le Normand, B. Villette, B. Raynal, J. Pungarčar, I. Križaj, I. G. Faure. *J. Struct. Biol.* **2010,** *169*, 360–369.
28. R. M. Kini, *Toxicon* **2005**, *45*, 1147–1161.
29. S. Stefansson, R. M. Kini, H. J. Evans, *Biochemistry* **1990**, *29*, 7742–7746.

30. M. Inada, R. M. Crowl, A. C. Bekkers, H. Verheij, J. Weiss, *J Biol Chem.* **1994,** *269,* 26338–26343.

31. S. Stefansson, R. M. Kini, H. J. Evans, *Thromb. Res.* **1989,** *55,* 481–491.

32. M. Perbandt, I-H. Tsai, A. Fuchs, S. Banumathi, K. R. Rajas-hankar, D. Georgieva, K. N. Kalkura, T. P. Singh, N. Genov, C. Betzel, *Acta Cryst.* **2003,** *D59,* 1679–1687.

33. E. Carredano, B. Westerlund, B. Persson, M. Saarinen, S. Ramaswamy, D. Eaker, H. Eklund, *Toxicon* **1998,** *36,* 75–92.

34. A. K. Sabharwal, K. Padmanabhan, A. Tulinsky, A Mathur, J. Gorka, S. P. Bajaj, *J. Biol. Chem.* **1997,** *272,* 22037–22045.

35. H. Brandstetter, M. Bauer, R. Huber, P. Lollar, W. Bode, *Proc. Natl. Acad. Sci.* USA **1995,** *92,* 9796–9800.

36. G. Faure, A. L. Harvey, E. Thomson, B. Saliou, F. Radvanyi, C. Bon, *Eur. J. Biochem.* **1993,** *214,* 491–496.

37. G. Faure, V. Choumet, C. Bouchier, L. Camoin, J. L. Guillaume, B. Monegier, M. Vuilhorgne, C. Bon, *Eur. J. Biochem.* **1994,** *223,* 161–164.

38. D. P. Marchi-Salvador, L. C. Corrêa, A. J. Magro, C. Z. Oliveira, A. M. Soares, M. R. Fontes, *Proteins* **2008,** *72,* 883–891.

39. B. Francis, A. Bdolah, I. I. Kaiser *Toxicon* **1995,** *33,* 863–74.

Povzetek

Nekatere fosfolipaze A$_2$ (PLA$_2$) kačjih strupov se z visoko afiniteto vežejo na človeški aktivirani faktor Xa (hFXa) v krvi in delujejo kot specifični, nekompetitivni inhibitorji strjevanja krvi. Zadnje določitve tridimenzionalnih struktur izooblik PLA$_2$, ki se razlikujejo v antikoagulantni aktivnosti, prispevajo k boljšemu razumevanju načina njihove vezave na hFXa. Podrobna analiza kristalnih struktur naravnih izooblik PLA$_2$ iz strupov viperidnih kač z različno afiniteto vezave na hFXa nam omogoča proučevanje lokalnih konformacijskih sprememb in natančno prepoznavanje ključnih aminokislinskih ostankov, pomembnih za antikoagulantno delovanje teh PLA$_2$. Tako smo v C-terminalni regiji PLA$_2$ s šibkejšim antikoagulantnim delovanjem (AtxC in CBa$_2$) zasledili konformacijske spremembe na mestu ohranjenega Lys127 na račun zamenjave sosednjega Lys128 > Glu, ki pomembno vplivajo na zmanjšanje afinitete do hFXa. Prav tako k zmanjšanju antikoagulantnega delovanja kompleksa CBa$_2$-FXa verjetno prispeva tudi zamenjava His1 > Ser v manj učinkovitem CBa$_2$, povezana z večjim premikom stranskih verig Lys69 in Trp70 v področju zanke 65–72. Poznavanje prostorske ureditve na mestih interakcije med PLA$_2$ in hFXa je pomembno za razumevanje procesa strjevanja krvi na molekulski ravni in lahko privede do razvoja novih antikoagulantnih zdravil.